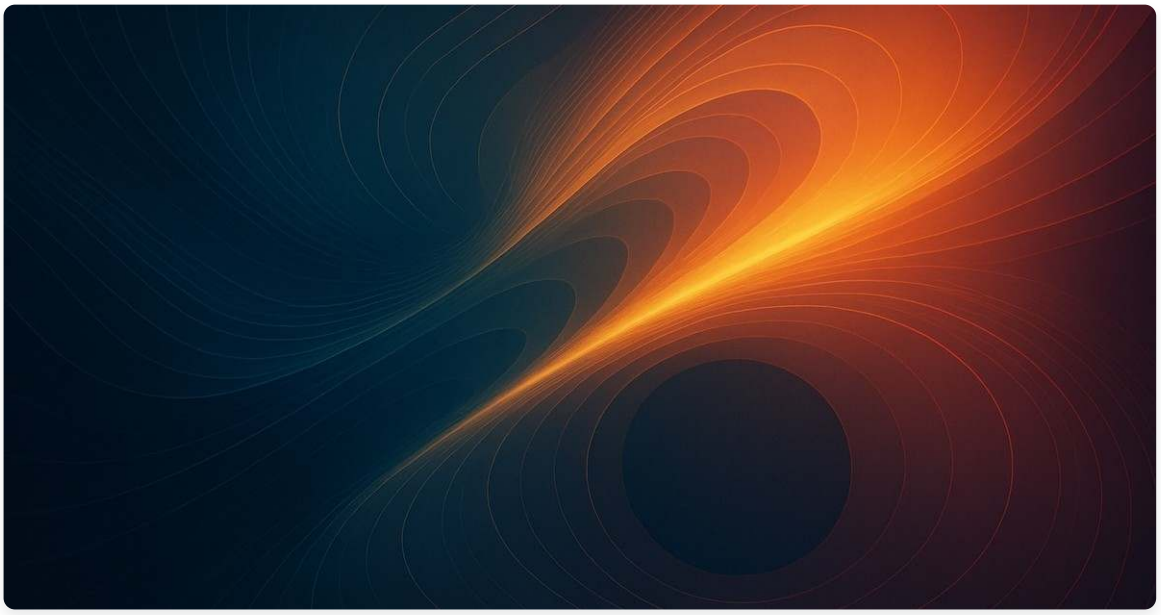

Temporal Equivalence Principle: Dynamic Time & Emergent Light Speed

Matthew Lukin Smawfield

Version: v0.9 (Jakarta)

First published: 18 August 2025 · Last updated: 6 June 2026

DOI: 10.5281/zenodo.16921911

Abstract

This paper proposes a covariant, testable reformulation of relativity in which proper time is a dynamical field and the "speed of light" is an emergent, strictly local invariant rather than a global constant. The framework is built on a single spacetime manifold endowed with two metrics: a gravitational metric $g_{\mu\nu}$ and a causal (matter) metric $\tilde{g}_{\mu\nu}$ to which all non-gravitational fields and clocks couple. The metrics are related by a controlled disformal map, $\tilde{g}_{\mu\nu} = A^2(\phi)g_{\mu\nu} + B(\phi)\nabla_\mu\phi\nabla_\nu\phi$, where ϕ is the time field, $A(\phi) = \exp(\beta_A\phi/M_{\rm Pl})$ is a universal conformal factor, and $B(\phi)$ encodes tiny, direction-dependent deformations of the light cone consistent with multi-messenger constraints ($|c_\gamma - c_g|/c \lesssim 10^{-15}$ today). Proper time is elevated to a field by postulating that all matter, electromagnetism, and quantum phases evolve with respect to $\tilde{g}$-proper time τ; in local freely falling frames, this guarantees exact local Lorentz invariance and a locally invariant c, while globally it implies that synchronization procedures and one-way light-time measurements become path-dependent in a dynamical-time background. The covariant action, field equations, conservation laws, Parametrized Post-Newtonian (PPN) mapping, and screening mechanisms are developed to reconcile terrestrial tests with cosmological dynamics. The breakdown of global simultaneity is formalized using a synchronization-transport law, deriving a convention-independent "synchronization holonomy," an invariant measure of non-integrability of time transport around closed loops. In the purely conformal subclass this holonomy vanishes after subtraction of the full GR, kinematic, clock-scale, and reference-frame synchronization model; nonzero holonomy at leading order requires residual non-exact synchronization structure, supplied in the minimal TEP model by disformal coupling $B(\phi) \neq 0$, and in more general extensions by non-metricity or other explicitly non-exact transport structure. Explicit small-B formulas are provided for the holonomy and the effective photon phase speed, showing how the measured one-way asymmetry is related to ϕ-gradients and disformal scales under current constraints. The analysis demonstrates that Einstein's assumption of a universal c was a brilliant local theorem arising from the Temporal Equivalence Principle; transcending it demands dynamical time: c remains exactly invariant locally, but global, one-way-inferred "c" values differ by path-dependent amounts that experiments can detect or bound. A staged, falsifiable experimental program is outlined: (1) a closed-loop, multi-leg, one-way time-transfer "triangle test" designed to detect synchronization holonomy at the 10^{-19} fractional level (after averaging) and subtracting known GR effects; (2) interplanetary one-way optical time transfer targeting picosecond-level asymmetries over AU baselines; (3) distance-correlation analysis and environment-dependent screening maps with precision clock networks; (4) multi-messenger searches for distance-correlated photon–gravitational-wave arrival differentials consistent with tightly bounded disformal propagation; (5) matter-wave interferometry and torsion-balance tests sensitive to environment-dependent couplings. Cosmologically, the time field can modify late-time distance and growth observables while preserving BBN and CMB acoustic physics in the screened early-time regime, potentially contributing to H_0 and S_8

phenomenology. Known weaknesses in the variable-c literature are addressed by supplying a correct, operationally invariant observable (holonomy), clarifying when conformal couplings cannot produce a signal, and providing realistic, constraint-consistent signal forecasts with explicit error budgets and statistical plans (pre-registration, blinding, publicly released code and data). The resulting theory preserves the empirical pillars of relativity (local Lorentz invariance, gravitational-wave causality, PPN bounds) while extending its conceptual foundation: simultaneity is not only relative but generally non-integrable; the speed of light is not a global constant but the local echo of a deeper, dynamical temporal geometry.

Long-standing confusions about "variable c" are resolved by replacing convention-dependent statements with invariant observables tied to measurement procedures. A synchronization one-form $\tilde{\sigma}$ is defined on spacelike slices of the matter metric; its curl $d\tilde{\sigma}$, after subtraction of the full GR, kinematic, clock-scale, and reference-frame synchronization model, yields a residual "temporal holonomy" H that vanishes in GR and becomes nonzero only when time is dynamical in this sense. Two key theorems are proven: (i) conformal matter coupling preserves null cones, so photons and gravitons share the same causal structure at late times; (ii) a static ϕ-gradient generates no first-order one-way light-time anisotropy, placing effects in the femto-to-picosecond regime over astronomical baselines under current bounds. Disformal tilts ($B \neq 0$) are tightly constrained by GW170817-class multi-messenger observations but can source holonomy at levels within reach of next-generation metrology. The covariant action is presented; field equations, conservation laws, invertibility/causality conditions, and a 3+1 decomposition are derived to make the observables explicit. Screening via a continuous Temporal Topology governed by non-linear superposition of field gradients (Temporal Shear) reconciles precision local tests with cosmological evolution, with mapping to Parametrized Post-Newtonian parameters and to the EFT-of-dark-energy α-functions with $c_T = 1$ enforced. Decisive experiments with quantitative error budgets are outlined: (1) a ground–ground–satellite triangle time-transfer experiment targeting holonomy at below 10^{-18} fractional after GR subtraction; (2) portable-clock "clock anholonomy" around closed paths at the 10^{-19} level over days; (3) multi-species clock networks seeking phase-locked annual modulations at 10^{-19}–10^{-17}; (4) interplanetary one-way optical links at picoseconds over AU; (5) altitude-dependent screening maps with optical clocks and atom interferometers; and (6) ensemble multi-messenger tests. A cosmological pipeline plan for CLASS/HyRec modifications and MCMC inference is provided, with commitment to open data and blinded analyses.

Einstein's postulate of universal c was a brilliant, operationally perfect approximation in regimes where time's flow is effectively uniform. In a universe where the rate of time is dynamical yet locally Lorentzian, "the speed of light" emerges as an invariant in every local lab but ceases to be globally universal. The new invariant content resides in path-dependent synchronization defects and holonomies of time transport, not in naive one-way "speeds." If detected, these invariants would inaugurate a post-Einsteinian era: from dynamic geometry to dynamic time.

1. Introduction: From a Universal Speed to a Universal Principle of Time

Relativity and quantum theory disagree about time. General relativity (GR) makes proper time geometric—$d\tau^2 = -g_{\mu\nu}dx^\mu dx^\nu/c^2$—dynamical, and observer-dependent. Quantum mechanics (QM) treats time as an external parameter t in the Schrödinger equation, $i\hbar\partial_t|\psi\rangle = \hat{H}|\psi\rangle$. The clash has haunted quantization programs for a century and manifested operationally as subtle ambiguities in defining one-way light speeds and simultaneity across extended regions. Precision clocks and time-transfer links now measure gravitational redshifts and velocity-dependent dilations at 10^{-18} fractional levels, while cosmology exhibits persistent H_0 and S_8 tensions. In this context, Einstein's postulate of a universal speed c must be sharpened: it is exact for any local freely falling laboratory, but it cannot be a global property if the flow of time itself is dynamical.

The Temporal Equivalence Principle (TEP) is proposed: all non-gravitational dynamics, signals, and quantum phases evolve according to the proper time defined by a single causal metric $\tilde{g}_{\mu\nu}$ that couples universally to matter. The rate at which proper time accrues is a field. This elevates "when" to the status "where" acquired in 1915: as space was geometrized, now time's rate is dynamized. The unavoidable consequence is that synchronization conventions are no longer globally integrable: even after removing known GR effects (Sagnac, Shapiro), closed-loop time transport does not necessarily return a clock to its initial epoch, and one-way times differ in opposite directions. The measured "speed of light" between distant clocks is revealed as an emergent ratio of distance to accrued proper time, not a fundamental constant comparable across regions without a theory of time's flow. Locally, c remains exactly invariant; globally, dynamical time imprints tiny, path-dependent asymmetries that can be detected or bounded.

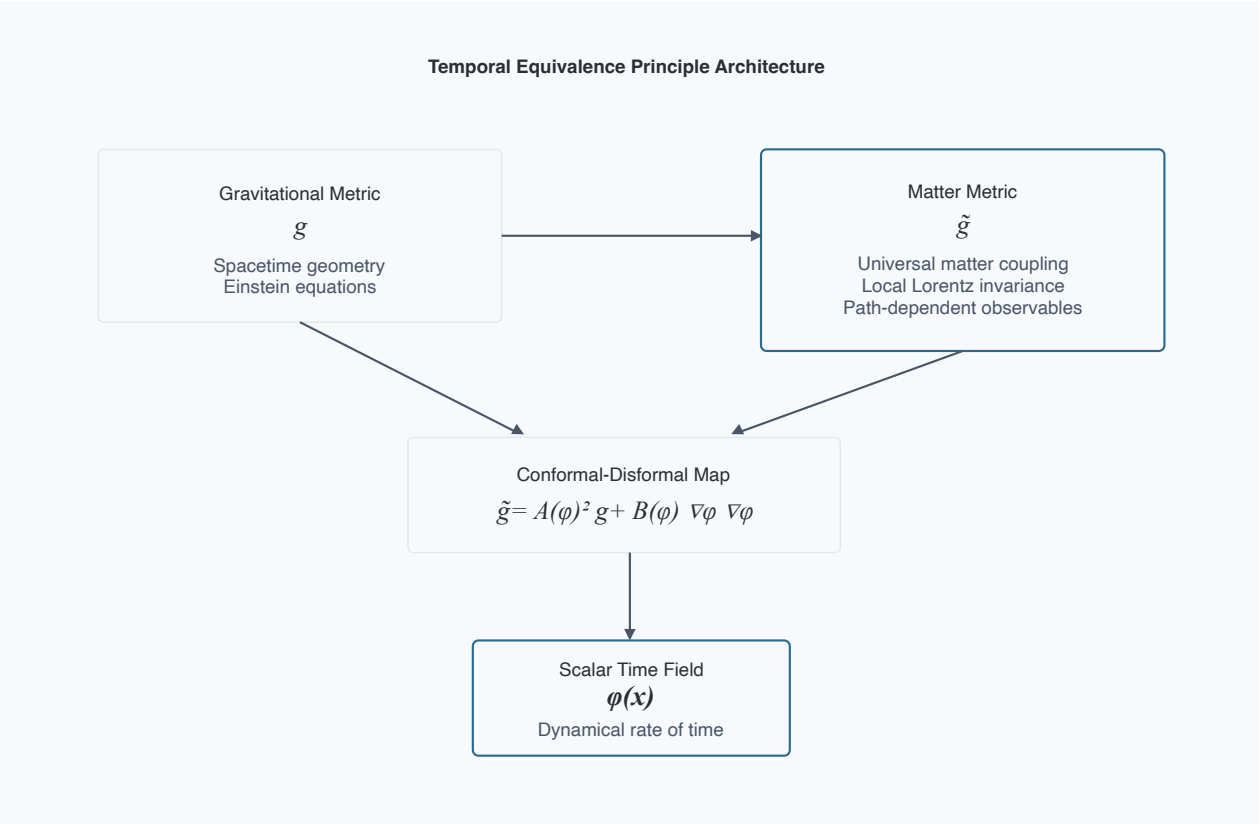

Figure 1. Temporal Equivalence Principle (TEP) architecture. Matter couples to $\tilde{g}_{\mu\nu}$ via a conformal–disformal map controlled by the scalar time field ϕ, preserving local Lorentz invariance while enabling new global invariants.

2. Axioms and the Temporal Equivalence Principle

The framework adopts four axioms:

A1. Two-metric structure on a single manifold. Gravity is described by a Lorentzian metric $g_{\mu\nu}$; matter fields, clocks, and rulers couple to a causal (matter) metric $\tilde{g}_{\mu\nu}$. The metrics are related by a disformal map

$$\tilde{g}_{\mu\nu} = A^2(\phi) g_{\mu\nu} + B(\phi) \nabla_\mu \phi \nabla_\nu \phi, \tag{1}$$

with a universal conformal factor $A(\phi) = \exp(\beta_A \phi / M_{\rm Pl})$ and a small disformal function $B(\phi)$ consistent with multi-messenger constraints today.

A2. Temporal Equivalence Principle (TEP). All non-gravitational processes evolve according to proper time $d\tau$ defined by $\tilde{g}_{\mu\nu}$: $i\hbar d|\psi\rangle/d\tau = \hat{H}|\psi\rangle$, nongravitational fields propagate on $\tilde{g}$-null cones, and ideal clocks tick $d\tau^2 = -\tilde{g}_{\mu\nu} dx^\mu dx^\nu / c^2$. In local freely falling frames for $\tilde{g}_{\mu\nu}$, physics reduces to special relativity with invariant c.

A3. Causal safety and locality. Today, $c_g = c_\gamma$ within current bounds ($|c_g - c_\gamma|/c \lesssim 10^{-15}$). This is enforced by choosing $A(\phi)$ universal, such that conformal transformations preserve null cones for photons and gravitons when $B = 0$, and by constraining the observable combination $B(\phi)(\partial\phi)^2$ along late-time astrophysical propagation paths. Different experiments constrain different integrals or responses involving the single disformal function $B(\phi)$; GW170817 does not require B to vanish identically in all regimes. Hyperbolicity and energy conditions hold within the EFT domain.

A4. Screening and universality. The coupling $A(\phi)$ is universal at leading order; loop-induced composition dependence is tightly bounded. Environmental suppression of the locally observable Temporal Shear/source-charge sector reconciles local tests with cosmological dynamics. Chameleon, Vainshtein, Galileon, DBI, and symmetron mechanisms are treated as candidate microscopic completions, not as the defining ontology of TEP. Screening manifests as a continuous spatial and covariance structure of the scalar time field (Temporal Topology) governed by the temporal potential field and its gradient (Temporal Shear), suppressing fifth forces in screened regimes while leaving cosmology accessible to dynamics.

These axioms encode Einstein's local invariance as a theorem and extend it: c is exactly invariant for every tangent space of $\tilde{g}_{\mu\nu}$, but global synchronization and one-way timing depend on the dynamical field ϕ.

Sector mapping

Sector	Physical effect	Coupling	Key bound
Conformal $A(\phi)$	Clock rates, proper time rescaling	Universal (β_A)	Cassini PPN-γ, redshift tests
Disformal $B(\phi)$	Null cone tilts, direction-dependent propagation	Small, environment-dependent	GW170817: $\lvert c_\gamma - c_g\rvert/c \lesssim 10^{-15}$
Temporal Topology	Spatial/covariance structure of $\ln A(\phi)$	Field configuration + gradient suppression	Clock/covariance correlation length λ_T

The conformal sector governs clock rates; the disformal sector governs cone tilts. GW170817 directly bounds disformal cone splits governed by B. It does not directly test common-mode conformal clock-rate structure governed by A, although local conformal gradients/source charges remain constrained by PPN, gravitational-redshift, clock-comparison, and equivalence-principle tests.

2.1 Relation to Other Modified Gravity Frameworks

The TEP framework can be situated within the broader landscape of modified gravity and scalar-tensor theories. To clarify its unique features, a comparative analysis is provided:

Table 1: Comparison with Other Scalar-Tensor Frameworks

Theory/Framework	Key Fields	Matter Coupling	$c_g = c_\gamma$?	Key Observable Signature
TEP (This work)	$g_{\mu\nu}$, ϕ	Universal to $\tilde{g}_{\mu\nu} = A^2 g_{\mu\nu} + B\partial_\mu\phi\partial_\nu\phi$	Equal in conformal/common-mode limit; differential deviations possible through B and constrained by same-path EM–GW timing	Synchronization Holonomy H_{resid}
Horndeski	$g_{\mu\nu}$, ϕ	Minimal to $g_{\mu\nu}$	Yes, after GW170817 constraints	Modified growth, ISW
DHOST	$g_{\mu\nu}$, ϕ	Minimal to $g_{\mu\nu}$	Yes, for specific degenerate classes	Modified growth, screening
TeVeS	$g_{\mu\nu}$, A_μ, ϕ	To a combined metric	No	MOND phenomenology, lensing
SMEFT	SM fields	Lorentz-violating operators	Model-dependent	Anisotropic propagation, CPT violation

The multi-messenger constraint from GW170817 constrains the integrated EM–GW differential disformal contribution along observed late-time astrophysical paths. It does not require the disformal sector to vanish identically in all regimes. In the conformal limit, common-mode path effects cancel in EM–GW timing; residual B-sector structure remains testable through multipath delays, closed-loop holonomy, and topological or interferometric regimes. The model, with a universal conformal coupling $A(\phi)$ and a disformal term $B(\phi)$, automatically satisfies $c_g = c_\gamma$ in the conformal limit ($B = 0$). A non-zero $B(\phi)$ introduces a calculable deviation $c_\gamma \neq c_g$ constrained by future multi-messenger observations.

Conceptually, TEP differs from many scalar-tensor theories by its foundational principle: the universal coupling of matter to a single metric $\tilde{g}_{\mu\nu}$. This is philosophically closer to Bekenstein's TeVeS theory, which also introduced a separate matter metric, but the framework is more minimal, using only a scalar, and makes a unique prediction in the form of the synchronization holonomy.

2.2 Minimal covariant action

The minimal EFT action used in this paper is

$$S = \int d^4x\sqrt{-g}\left[\frac{M_{\rm Pl}^2}{2}R - \frac{1}{2}(\nabla\phi)^2 - V(\phi)\right] + S_m[\psi_i, \tilde{g}_{\mu\nu}], \tag{2}$$

with

$$\tilde{g}_{\mu\nu} = A^2(\phi) g_{\mu\nu} + B(\phi) \nabla_\mu \phi \nabla_\nu \phi. \tag{3}$$

Variation with respect to the Einstein-frame metric, ϕ, and matter fields gives the Einstein-frame field equations, scalar equation of motion, and matter-frame conservation law.

2.3 Field equations and conservation laws

Varying the action with respect to the Einstein-frame metric, ϕ, and the matter fields yields three sets of equations.

Einstein-frame field equations

$$G_{\mu\nu} = \frac{1}{M_{\rm Pl}^2} \left[T^{(\phi)}_{\mu\nu} + T^{(m)}_{\mu\nu} \right], \tag{4}$$

with the scalar stress-energy

$$T^{(\phi)}_{\mu\nu} = \nabla_\mu \phi \nabla_\nu \phi - g_{\mu\nu} \left[\frac{1}{2} (\nabla\phi)^2 + V(\phi) \right]. \tag{5}$$

The Einstein-frame matter stress-energy $T^{(m)}_{\mu\nu}$ is obtained from $S_m[\tilde{g}]$ by functional differentiation with respect to the inverse Einstein-frame metric $g^{\mu\nu}$:

$$T^{(m)}_{\mu\nu} = -\frac{2}{\sqrt{-g}} \frac{\delta S_m}{\delta g^{\mu\nu}} = \frac{\sqrt{-\tilde{g}}}{\sqrt{-g}} \, \tilde{T}^{(m)}_{\alpha\beta} \, \frac{\partial \tilde{g}^{\alpha\beta}}{\partial g^{\mu\nu}}, \tag{6}$$

where $\tilde{T}^{(m)}_{\alpha\beta} = -\frac{2}{\sqrt{-\tilde{g}}} \frac{\delta S_m}{\delta \tilde{g}^{\alpha\beta}}$ is the matter-frame stress-energy. For the disformal inverse

$$\tilde{g}^{\mu\nu} = A^{-2} \left[g^{\mu\nu} - \frac{(B/A^2) \, \partial^\mu \phi \, \partial^\nu \phi}{1 + (B/A^2)(\partial\phi)^2} \right], \tag{7}$$

the Jacobian $\partial \tilde{g}^{\alpha\beta} / \partial g^{\mu\nu}$ yields, at leading order in small B,

$$T^{(m)}_{\mu\nu} = A^2(\phi) \, \tilde{T}^{(m)}_{\mu\nu} + O(B). \tag{8}$$

Thus the Einstein-frame equations reduce to a scalar-tensor theory with conformally-coupled matter at leading order; disformal corrections enter at $O(B)$ and are suppressed by the same multi-messenger bounds that constrain the light-cone tilt.

Scalar equation of motion

For the scalar equation it is useful to define the matter-frame stress tensor by

$$\tilde{T}^{\mu\nu} \equiv \frac{2}{\sqrt{-\tilde{g}}} \frac{\delta S_m}{\delta \tilde{g}_{\mu\nu}}. \tag{9}$$

This is equivalent to the covariant definition

$$\tilde{T}_{\mu\nu} = -\frac{2}{\sqrt{-\tilde{g}}}\frac{\delta S_m}{\delta \tilde{g}^{\mu\nu}}, \tag{10}$$

with indices raised and lowered using $\tilde{g}_{\mu\nu}$.

We also define the density-weighted tensor

$$\mathcal{T}^{\mu\nu} \equiv \frac{\sqrt{-\tilde{g}}}{\sqrt{-g}}\tilde{T}^{\mu\nu}. \tag{11}$$

Varying the matter metric with respect to ϕ gives

$$\delta_\phi \tilde{g}_{\mu\nu} = 2AA_{,\phi} g_{\mu\nu}\delta\phi + B_{,\phi}\nabla_\mu\phi\nabla_\nu\phi\,\delta\phi + B\left(\nabla_\mu\delta\phi\,\nabla_\nu\phi + \nabla_\mu\phi\,\nabla_\nu\delta\phi\right). \tag{12}$$

After integrating the derivative terms by parts, the scalar equation can be written as

$$\Box\phi - V_{,\phi} = -\mathcal{Q}, \tag{13}$$

where

$$\mathcal{Q} = AA_{,\phi} g_{\mu\nu}\mathcal{T}^{\mu\nu} + \frac{1}{2}B_{,\phi}\mathcal{T}^{\mu\nu}\nabla_\mu\phi\nabla_\nu\phi - \nabla_\mu\left(B\mathcal{T}^{\mu\nu}\nabla_\nu\phi\right). \tag{14}$$

Equivalently,

$$\Box\phi = V_{,\phi} - AA_{,\phi} g_{\mu\nu}\mathcal{T}^{\mu\nu} - \frac{1}{2}B_{,\phi}\mathcal{T}^{\mu\nu}\nabla_\mu\phi\nabla_\nu\phi + \nabla_\mu\left(B\mathcal{T}^{\mu\nu}\nabla_\nu\phi\right). \tag{15}$$

In the conformal limit $B \to 0$, this reduces to the standard conformally coupled scalar-tensor source equation,

$$\Box\phi - V_{,\phi} = -AA_{,\phi} g_{\mu\nu}\mathcal{T}^{\mu\nu}. \tag{16}$$

Equivalently, in terms of the effective scalar coupling

$$\alpha(\phi) \equiv \frac{d\ln A}{d\phi}, \tag{17}$$

the conformal source is proportional to the matter trace. Nonrelativistic matter sources the scalar through $T \simeq -\rho$, while radiation with $T \simeq 0$ weakly sources the conformal sector, as used in the cosmological discussion.

Matter-frame conservation law

$$\tilde{\nabla}_\mu \tilde{T}^{\mu\nu}_{(m)} = 0, \tag{18}$$

which follows from diffeomorphism invariance of $S_m[\tilde{g}]$ and implies that non-gravitational test particles and light follow geodesics of the matter metric $\tilde{g}_{\mu\nu}$. In the Einstein frame, matter and the scalar exchange energy-momentum. Diffeomorphism invariance gives

$$\nabla_\mu T^{\mu\nu}_{(m)} = \mathcal{Q}\nabla^\nu \phi, \tag{19}$$

while the scalar stress tensor satisfies

$$\nabla_\mu T^{\mu\nu}_{(\phi)} = -\mathcal{Q}\nabla^\nu \phi. \tag{20}$$

Therefore the total Einstein-frame stress tensor is conserved:

$$\nabla_\mu \left(T^{\mu\nu}_{(m)} + T^{\mu\nu}_{(\phi)} \right) = 0. \tag{21}$$

The matter-frame conservation law remains

$$\tilde{\nabla}_\mu \tilde{T}^{\mu\nu}_{(m)} = 0, \tag{22}$$

because matter is minimally coupled to $\tilde{g}_{\mu\nu}$.

These equations define the EFT structure used throughout the paper. The scalar source $\mathcal{Q}$ displays the leading conformal-disformal matter coupling explicitly.

3. Operational Foundations: Measurement, Simultaneity, and One-Way Light

3.1 What is actually measured

No measurement of c uses null proper time along the photon's worldline; that would be $c = dx/d\tau$ with $d\tau = 0$. Instead, a distance is compared with an elapsed proper time on an observer's clock. For two spatially separated clocks A and B with worldlines γ_A, γ_B and a light path λ from A to B, the measured one-way time t_{AB} is the difference in B's proper time between emission and reception, after a synchronization convention has assigned simultaneity between A and B. Two-way measurements are convention-independent; one-way measurements are not, unless an invariant observable is provided.

3.2 The synchronization problem in a dynamical-time background

Einstein synchronization assumes (i) reciprocity of propagation and (ii) homogeneity of time standards along the path. If the rate $d\tau/dt$ varies spatially or directionally, synchronization by light exchange over extended loops becomes path-dependent. The proper formalism invokes the congruence u_μ of observers (clocks) and the null geodesics k^μ of $\tilde{g}_{\mu\nu}$. Define simultaneity as orthogonality to u_μ (where Frobenius integrability allows it), and define time transport by mapping a proper-time interval at A to B using $\tilde{g}$-null signals. In GR, the non-closure of such transports arises from rotation of the congruence (vorticity) and spacetime curvature (Sagnac/Shapiro); both can be modeled and removed. In a dynamical-time geometry with disformal couplings, there is an additional, tiny non-exact contribution to time transport that cannot be removed by coordinate choices: a synchronization holonomy.

3.3 A convention-independent observable: synchronization holonomy

The operational observable is not a raw one-way speed and not the integral of a scalar proper-time differential. It is the residual non-closure of synchronization transport around a closed loop after subtracting the GR prediction.

Let $\tilde{\sigma}$ denote the matter-frame synchronization transport one-form induced by $\tilde{g}_{\mu\nu}$ and the chosen clock congruence, and let σ_{GR} denote the corresponding GR one-form including Sagnac, gravitomagnetic / Lense–Thirring, Shapiro delay, gravitational redshift, station motion, clock-scale realization, and reference-frame corrections. The residual holonomy is:

$$H_{\mathrm{resid}}(C) \equiv \oint_C (\tilde{\sigma} - \sigma_{\mathrm{GR}}) = \iint_\Sigma (d\tilde{\sigma} - d\sigma_{\mathrm{GR}}), \qquad C = \partial\Sigma. \tag{23}$$

Equivalently, defining $\tilde{F} = d\tilde{\sigma}$ and $F_{\mathrm{GR}} = d\sigma_{\mathrm{GR}}$:

$$H_{\mathrm{resid}}(C) = \iint_\Sigma (\tilde{F} - F_{\mathrm{GR}}). \tag{24}$$

This quantity is invariant under admissible synchronization re-gaugings because the matter-frame connection $\tilde{\sigma}$ and the corresponding GR reference connection σ_{GR} shift by the same exact one-form, leaving the residual connection $\Delta\sigma = \tilde{\sigma} - \sigma_{\mathrm{GR}}$ unchanged. Equivalently, any representative shift by an exact form integrates to zero around a closed loop.

Conformal exactness and vanishing loop holonomy

In the conformal-only subclass ($B = 0$), the scalar contribution to local clock-rate transport is generated by the exact one-form $\omega^{(A)} = d\ln A$. For any closed loop C in a simply connected region where $A(\phi)$ is smooth and single-valued:

$$\oint_C \omega^{(A)} = \oint_C d\ln A = 0. \tag{25}$$

Thus a conformal-only scalar may affect local rates and open-path redshift comparisons, but it cannot by itself generate a closed-loop residual synchronization holonomy. A leading-order nonzero H_{resid} requires residual synchronization curvature $d(\tilde{\sigma} - \sigma_{\mathrm{GR}}) \neq 0$, which in this framework arises from the disformal sector, non-metricity, or other explicitly non-exact transport structure.

This reframes "variable c" claims: the invariant diagnostic is not a raw one-way c, but H_{resid}. A nonzero H_{resid} means simultaneity is not integrable beyond GR; this is what dynamic time does to measurement.

Figure 2. Synchronization holonomy on a spacelike slice in the matter frame. The residual invariant H_{resid} subtracts all GR corrections (Sagnac, gravitomagnetic / Lense–Thirring, Shapiro delay, gravitational redshift, station motion, clock-scale realization, and reference-frame corrections), isolating dynamical-time effects.

4. Disformal Invertibility, Causality, and Hyperbolicity

Invertibility and signature

The inverse of $\tilde{g}_{\mu\nu}$ exists for $A > 0$ and $1 + (B/A^2)(\partial\phi)^2 \neq 0$:

$$\tilde{g}^{\mu\nu} = A^{-2}\left[g^{\mu\nu} - \frac{(B/A^2)\partial^\mu\phi\partial^\nu\phi}{1 + (B/A^2)(\partial\phi)^2}\right]. \tag{26}$$

For Lorentzian signature, require $A > 0$ and $B(\partial\phi)^2 > -A^2$. B is assumed small and gradients bounded in all regimes of interest.

Causality

The matter cone is inside or equal to the gravitational cone when $B \geq 0$ and gradients are modest; no closed causal curves arise for small B. With $B \to 0$ at late times, gravitational and matter null cones coincide ($c_T = c_{\mathrm{EM}}$). With B small, any phase differences in propagation are minute and bounded by multi-messenger results.

Hyperbolicity

The scalar's canonical kinetic ensures hyperbolic evolution with well-posed Cauchy problem where $V''(\phi) > 0$ near minima. Maxwell's equations in a Lorentzian matter metric remain hyperbolic. Linearized gravity propagates on the Einstein-frame cone. Within the small-B, canonical-scalar EFT regime considered here, no ghost or gradient instability is introduced at leading order. The EFT is valid below the disformal scale M, with higher-dimensional operators suppressed.

5. Local Lorentz Invariance, Proper Time, and the Emergence of c

Proper time

Clocks measure $d\tau^2 = -\tilde{g}_{\mu\nu}dx^\mu dx^\nu/c^2$. In a local lab with small velocities and $\partial_0\phi \ll |\nabla\phi|$, $-\tilde{g}_{00} \approx A(\phi)^2(-g_{00}) - B(\partial_0\phi)^2$, so

$$\frac{d\tilde{\tau}}{d\tau_g} = A(\phi), \tag{27}$$

up to $O(B)$ corrections. This "dynamical time law" rescales all frequency standards locally.

Local c

All small labs measure an invariant c; the conformal factor rescales both clocks and rulers uniformly, preserving null cones. Thus the empirical fact "c is constant" remains a theorem of the theory at the local level.

Global measures

Global "speeds" involve synchronized endpoints. Because $d\tau$ depends on ϕ's history, the global assignment of simultaneity acquires non-integrability when ϕ varies in space or time. That non-integrability—not a local violation of Lorentz invariance—is the source of observable departures.

6. Synchronization in a Dynamical Time: One-Way Light and Holonomy

Operational definitions

Two-way light speed is synchronization-independent and has established c's local invariance. One-way measures require synchronized clocks at A and B; Einstein synchronization assumes time-orthogonal slices and propagation symmetry. In a dynamical ϕ background, slow clock transport and one-way synchronization are path and history dependent.

Key theorems

Theorem 1 (Conformal null-cone invariance)

For $\tilde{g}_{\mu\nu} = A(\phi)^2 g_{\mu\nu}$, null vectors of $g_{\mu\nu}$ are null for $\tilde{g}_{\mu\nu}$. Maxwell's action is conformally invariant in 4D, so photon trajectories are null with respect to both metrics. Gravitational and electromagnetic waves share null cones when $B = 0$ at late times.

Theorem 2 (No first-order one-way anisotropy in static φ)

For static ϕ with $\partial_0\phi = 0$, the one-way light-time difference for forward/backward propagation along the same path cancels to first order in $\nabla\phi$. Any residual is $O((\nabla\phi)^2)$ or due to time dependence/kinematics. Over astronomical baselines and with current bounds on $\alpha \equiv d\ln A/d\phi$, this places effects in the femto-to-picosecond regime, removing claims of microsecond-scale anomalies.

> ***Proof sketch.*** *Parameterize the path coordinate $s \in [0, L]$; write $t_{\rightarrow} = \int ds A(\phi_0 + s\partial_{\parallel}\phi)/c$ and $t_{\leftarrow}$ similarly along the reverse. Linear terms in $\partial_{\parallel}\phi$ cancel exactly; see Appendix A2 for full derivation.*

Synchronization one-form and holonomy

Decompose $\tilde{g}_{\mu\nu}$ in 3+1 form:

$$\tilde{g}_{\mu\nu}dx^\mu dx^\nu = -\tilde{N}^2 dt^2 + \tilde{h}_{ij}(dx^i + \tilde{N}^i dt)(dx^j + \tilde{N}^j dt). \tag{28}$$

Define the coordinate synchronization connection by the threading representative

$$\tilde{\sigma}_i = \frac{\tilde{g}_{0i}}{\tilde{g}_{00}}, \tag{29}$$

up to the overall sign convention adopted for simultaneity transport. In ADM variables, for small shift,

$$\tilde{\sigma}_i \simeq -\frac{\tilde{N}_i}{\tilde{N}^2}. \tag{30}$$

A proper-time-normalized representative differs by a factor of the lapse; all closed-loop observables below use the same representative for both $\tilde{\sigma}$ and σ_{GR}, so the GR-subtracted residual is unaffected by this normalization choice. For a closed spatial loop C, the raw loop integral is

$$H = \oint_C \tilde{\sigma}, \tag{31}$$

but the physical TEP observable is the GR-subtracted residual

$$H_{\mathrm{resid}}(C) = \oint_C (\tilde{\sigma} - \sigma_{\mathrm{GR}}) = \iint_\Sigma (d\tilde{\sigma} - d\sigma_{\mathrm{GR}}), \qquad C = \partial\Sigma. \tag{32}$$

In GR with stationary spacetimes, the raw holonomy reproduces the Sagnac/gravito-magnetic effect; these known contributions are subtracted using geodesy and ephemerides. The residual holonomy beyond GR is therefore

$$H_{\mathrm{resid}}(C) = \iint_\Sigma (d\tilde{\sigma} - d\sigma_{\mathrm{GR}}), \qquad C = \partial\Sigma, \tag{33}$$

where σ_{GR} includes the standard Sagnac, gravitomagnetic/Lense--Thirring, Shapiro, gravitational-redshift, station-motion, clock-scale, and reference-frame contributions. This residual vanishes in SR/GR with $B = 0$ and stationary A; it is generically nonzero with disformal corrections ($B \neq 0$) and/or temporal variation of A combined with motion through $\nabla\phi$. Configurations in which C does not bound a smooth surface — non-simply-connected transport, or a connection that is locally closed but not globally exact — are not described by this Stokes expression and are treated as a separate topological case in Appendix A3.

Gauge and protocol invariance

$\tilde{\sigma}$ and σ_{GR} are synchronization-connection representatives for the same physical clock network and the same loop, evaluated in the matter-frame model and the corresponding GR reference model respectively. A synchronization re-gauging $t \to t + \chi(x^i)$ shifts both representatives by the same exact one-form. Therefore the GR-subtracted connection

$$\Delta\sigma = \tilde{\sigma} - \sigma_{\mathrm{GR}} \tag{34}$$

and its closed-loop integral

$$H_{\mathrm{resid}}(C) = \oint_C \Delta\sigma \tag{35}$$

are invariant under admissible synchronization changes. This addresses the critique that holonomy is conventional: the observable is the residual loop class of $\Delta\sigma$, not the exact part of any raw one-way synchronization convention.

Disformal corrections to $\tilde{\sigma}$

For small B and modest $\partial\phi$,

$$\tilde{N} \approx AN\left[1 - \frac{B}{2A^2N^2}(n\cdot\partial\phi)^2\right], \quad \tilde{N}_i \approx A\left[N_i + \frac{B}{A^2}(\partial_i\phi)(n\cdot\partial\phi)\right], \tag{36}$$

with n^μ the unit normal to slices. Then $\delta\tilde{\sigma}$ denotes the leading disformal correction to the chosen synchronization representative. Its covariant clock-congruence form is derived in Appendix A3; in a hypersurface-orthogonal $3+1$ slicing it reduces, up to lapse/shift convention and overall sign, to the expression proportional to

$$-\frac{B}{A^2N}(\partial_i\phi)(n\cdot\partial\phi)\,dx^i. \tag{37}$$

At leading order beyond the GR-subtracted reference model,

$$d(\Delta\sigma) = d(\tilde{\sigma} - \sigma_{\mathrm{GR}}) \supset d(\delta\tilde{\sigma}), \tag{38}$$

where the Δ indicates the residual beyond GR. Time dependence of ϕ and motion through $\nabla\phi$ generate non-vanishing curl.

7. Screening, PPN, Equivalence Principle, and Disformal Bounds

Screening

Screening in TEP is described as suppression of the locally observable Temporal Shear/source-charge sector, not as a commitment to a specific chameleon, Vainshtein, Galileon, DBI, or symmetron microphysics. Those mechanisms may be studied as candidate completions. In the effective theory used here, screening is expressed through the conformal factor $\ln A(\phi)$, its gradient Σ_μ, and its covariance C_A (compactly denoted Θ, C_Θ where convenient). Source structure, environmental state, and boundary conditions suppress the locally active shear sector in screened regimes.

The saturation scale ρ_T denotes the Temporal Topology saturation scale. It is not a local on/off condition of the form $\rho > \rho_T \Rightarrow$ GR and $\rho < \rho_T \Rightarrow$ active. Recovery of GR in local tests is controlled by suppression of the observable shear/source-charge sector, $\Sigma_\mu^{\mathrm{obs}} = \mathcal{S}_\Sigma(\mathcal{E})\Sigma_\mu$ with $\mathcal{S}_\Sigma \to 0$ in screened regimes, where $\mathcal{E}$ includes source structure, environment, boundary conditions, and density.

Temporal Topology and Temporal Shear: Canonical Formulation

The screening ontology is organized through a sector dictionary. The Temporal Shear is defined as the gradient of the conformal factor:

$$\Sigma_\mu \equiv \nabla_\mu \ln A(\phi) = \frac{\partial \ln A}{\partial\phi}\nabla_\mu\phi = \alpha(\phi)\nabla_\mu\phi, \tag{39}$$

where $\alpha(\phi) \equiv d(\ln A)/d\phi$ is the conformal coupling strength. For compactness one may write $\Theta \equiv \ln A$, but the canonical series notation remains $\ln A$, $\Sigma_\mu = \nabla_\mu \ln A$, and C_A.

The Temporal Topology correlation function $C_A(x, x')$ characterizes correlations of conformal-factor fluctuations:

$$C_A(x,x') \equiv \langle \delta \ln A(x)\, \delta \ln A(x') \rangle, \tag{40}$$

also denoted $C_\Theta(x,x') \equiv C_A(x,x')$ when using the compact notation. It is measured through clock/covariance data.

The temporal correlation length λ_T is the characteristic scale extracted from $C_A(x,x')$ in covariance measurements, not a derived algebraic combination of local fields.

The temporal saturation scale ρ_T is the characteristic scale at which Temporal Topology effects saturate in screening; it is a property of the theory's non-linear regime, not a local temporal energy density.

Finally, the observable response of any measurement channel X is parameterized by response coefficients κ_X:

$$\Delta O_X = \kappa_X \cdot \mathcal{S}_X(\mathcal{E}) \cdot \mathcal{F}_X[\Delta \ln A, \Sigma_\mu, C_A; \Phi, \rho, z], \tag{41}$$

where κ_X is an observable response coefficient for channel X, not the microscopic conformal coupling β_A and not a PPN coupling. The locally active PPN coupling is suppressed by the environmental/source screening factor $\mathcal{S}_\Sigma(\mathcal{E})$ and should not be confused with channel response coefficients κ_X.

PPN mapping

In unscreened regimes, the PPN parameter $\gamma_{\rm PPN} - 1 \approx -2\alpha_0^2/(1+\alpha_0^2) \approx -2\alpha_0^2$ with $\alpha_0 = \alpha(\phi_\infty)$; Cassini's $|\gamma_{\rm PPN} - 1| < 2.3 \times 10^{-5}$ implies $\alpha_0 \lesssim 3 \times 10^{-3}$. Near massive bodies, the suppression of Temporal Shear (vanishing field gradient) suppresses the effective scalar coupling to $\alpha_{\rm eff} \ll \alpha_0$, cleanly preserving PPN bounds without invoking rigid thin-shell approximations.

PPN recovery in the screened limit (DEF framework). In the Damour–Esposito-Farèse parameterization, the Jordan-frame metric for a static, spherically symmetric source is

$$g_{00}^{\rm J} = -1 + \frac{2GM}{r}\left(1 + \frac{\alpha_{\rm eff}^2}{2}\right), \quad g_{rr}^{\rm J} = 1 + \frac{2GM}{r}\left(1 - \frac{\alpha_{\rm eff}^2}{2}\right), \tag{42}$$

where $\alpha_{\rm eff}$ is the effective scalar charge that sources the exterior metric perturbation. For $A(\phi) = \exp(\beta_A \phi / M_{\rm Pl})$, the bare derivative $d(\ln A)/d\phi = \beta_A / M_{\rm Pl}$ is constant; screening does not make this derivative vanish. Instead, screening suppresses the effective exterior charge through the environmental screening factor:

$$\alpha_{\rm eff} = \mathcal{S}_\Sigma(\mathcal{E})\, \alpha_0, \tag{43}$$

where $\mathcal{S}_\Sigma(\mathcal{E}) \to 0$ in dense environments. When $\mathcal{S}_\Sigma \to 0$, the effective coupling $\alpha_{\rm eff} \to 0$ and the PPN parameters reduce exactly to GR values:

$$\gamma_{\rm PPN} - 1 = -2\alpha_{\rm eff}^2 \to 0, \qquad \beta_{\rm PPN} - 1 = \frac{\alpha_{\rm eff}^2}{2}\frac{d\alpha_{\rm eff}}{d\phi} \to 0. \tag{44}$$

Thus $\gamma_{\rm PPN} = \beta_{\rm PPN} = 1$ in the screened limit, independent of the cosmological value α_0.

Equivalence principle

TEP ensures universality in the matter frame. In the Einstein frame, the apparent fifth force is bounded by Eötvös experiments; MICROSCOPE gives $\eta \lesssim 10^{-14}$. Sectoral dilaton-like couplings (to α, μ, quark masses) are constrained to $|d| \lesssim 10^{-5}$–10^{-6} by composition tests and clock ratios.

Disformal constraints

GW170817/GRB170817A constrain $|c_\gamma - c_g|/c \lesssim \text{few} \times 10^{-15}$ at $z \approx 0.01$, bounding the observable combination $B(\phi)(\partial\phi)^2$ along the observed astrophysical path. This does not require B to vanish identically. In regimes where common-mode conformal effects dominate, B may remain active as a source for synchronization holonomy, multipath propagation anomalies, or interferometric signatures without violating the same-path EM–GW timing bound.

Disformal holonomy and the screening ontology

As established in Section 3.3, the invariant synchronization observable is the GR-subtracted residual

$$H_{\rm resid}(C) = \oint_C \Delta\sigma, \qquad \Delta\sigma \equiv \tilde{\sigma} - \sigma_{\rm GR}. \tag{45}$$

In the conformal-only subclass, the scalar clock-rate contribution is the exact one-form $d\ln A$, so it cannot by itself generate closed-loop residual synchronization holonomy in a smooth simply connected region. A leading-order nonzero $H_{\rm resid}$ requires residual synchronization curvature,

$$d\Delta\sigma \neq 0. \tag{46}$$

In the minimal TEP model this curvature is supplied by the disformal sector; in more general extensions it may arise from non-metricity or other explicitly non-exact transport structure.

To state the disformal contribution in a measurement-defined way, let u^μ denote the four-velocity field of the physical clock network or observer congruence used to define the synchronization protocol. We use the $(-+++)$ signature, so that

$$u^\mu u_\mu = -1. \tag{47}$$

Let

$$P_\mu{}^\nu = \delta_\mu{}^\nu + u_\mu u^\nu \tag{48}$$

be the spatial projector into the local rest space of that congruence. To leading order in the disformal correction, the projected contribution to the synchronization connection has the representative form

$$\delta\tilde{\sigma}_\mu \simeq -\frac{B}{A^2}(u\cdot\nabla\phi)P_\mu{}^\nu\nabla_\nu\phi, \tag{49}$$

up to the sign convention used for the synchronization one-form and higher-order disformal corrections.

Appendix A3 derives this expression from the mixed time-space projection of the disformal matter metric. It also shows that synchronization re-gaugings shift both the matter-frame synchronization connection and the corresponding GR reference connection by the same exact one-form. Therefore the GR-subtracted residual connection $\Delta\sigma$ is invariant under synchronization convention changes, and

$$H_{\rm resid}(C) = \oint_C \Delta\sigma \tag{50}$$

is independent of the arbitrary simultaneity convention used to coordinatize the specified physical clock network.

The invariant claim is therefore precise: $H_{\rm resid}$ is not independent of which physical clock network is used, but for a specified physical clock-network protocol it is independent of arbitrary synchronization re-labelling.

For a hypersurface-orthogonal clock network, $u^\mu = n^\mu$, the projected expression reduces to the familiar $3+1$ form

$$\delta\tilde{\sigma}_i \approx -\frac{B}{A^2 N}(\partial_i\phi)(n\cdot\partial\phi), \tag{51}$$

where N is the lapse and n^μ is the unit normal to the spatial slices. This ADM expression should be read as a special-case representation of the physical congruence formulation, not as the definition of the observable.

Unlike $d\ln A$, the disformal contribution is not generically exact. In the local non-topological case, its curvature satisfies

$$d(\delta\tilde{\sigma}) \neq 0 \tag{52}$$

whenever the prefactor multiplying the projected scalar gradient varies independently around the loop, for example through time dependence, anisotropic boundary conditions, inhomogeneous field structure, lapse/shift structure, or spatial variation of the disformal response within a fixed physical clock-network protocol. For a loop C bounding a smooth surface Σ, the local non-exact contribution to the residual holonomy may be written

$$H_{\rm resid}(C) = \oint_C \Delta\sigma = \iint_\Sigma d(\Delta\sigma). \tag{53}$$

At leading order beyond the GR-subtracted reference model, $d(\Delta\sigma)$ contains the disformal curvature $d(\delta\tilde{\sigma})$. Topological holonomy, where the loop does not bound a smooth surface or the connection is locally closed but not globally exact, is a separate case and is not represented by the Stokes expression above.

This also clarifies the screening ontology. The conformal and disformal sectors are correlated through the same scalar field ϕ, but their observable responses need not be assumed identical. Macroscopic screening suppresses the observable conformal shear,

$$\Sigma_\mu^{\rm obs} = \mathcal{S}_\Sigma(\mathcal{E})\Sigma_\mu, \tag{54}$$

thereby driving local clock-rate deviations toward the GR limit. In the limiting case where screening drives all scalar gradients to zero, the disformal holonomy also vanishes. However, the relation between conformal screening and disformal screening is not fixed by the conformal sector alone. It depends on the field solution, the disformal coupling $B(\phi)$, the physical clock-network congruence, boundary conditions, and probe-specific response.

Accordingly, high-energy, mesoscopic, and topological probes should not be modeled solely by the ambient bulk-density screening function used in astrophysical applications. Their responses are represented by channel-specific coefficients κ_X, depending on momentum transfer, interaction topology, boundary geometry, and microscopic field structure. These probes test whether non-exact disformal transport remains measurable in regimes where the conformal clock-rate response is screened.

8. Cosmology: Background Evolution, Growth, and EFT Mapping

Background

In spatially flat FLRW (Einstein frame),

$$3M_{\rm Pl}^2H^2 = \rho_m + \rho_r + \rho_\phi, \tag{55}$$

$$\ddot{\phi} + 3H\dot{\phi} + V'(\phi) = -\alpha(\phi)\rho_m + O(B), \tag{56}$$

$$\dot{\rho}_m + 3H\rho_m = +\alpha(\phi)\dot{\phi}\rho_m, \tag{57}$$

$$\dot{\rho}_r + 4H\rho_r = 0. \tag{58}$$

In the matter frame, the continuity equation for $\tilde{\rho}_m$ is standard; the Einstein-frame exchange encodes energy flow between ϕ and matter. During radiation domination, $T \approx 0$ and ϕ is overdamped; it thaws during matter domination. Under a standard FLRW/EFT reconstruction

this late-time temporal sector can be parameterized as an effective dark-energy component, but in TEP ontology it is not a fundamental dark-energy substance.

EFT of dark energy mapping

The theory maps to EFT-of-DE with $\alpha_T = 0$ enforced to satisfy $c_T = 1$. The braiding α_B and Planck-mass run α_M are both small and controlled by $\alpha(\phi)$ and $\dot{\phi}$. Bounds from large-scale structure and ISW require $|\alpha_M|, |\alpha_B| \ll 1$ at late times. The parameter choices respect these.

Recombination and H_0

In the current CMB-preserving realization, the early homogeneous temporal-shear mode is frozen or suppressed before recombination by the exponential transition function $S(z) = \exp[-(z/z_T)^{n_T}]$, preserving the sound horizon r_s and acoustic morphology to sub-percent precision. The homogeneous amplitude ϵ_T is driven to the ΛCDM limit by Planck acoustic anchors, with $\epsilon_T \approx 0$ at $z \sim 1100$. Sectoral couplings d_e at recombination must be tiny to preserve α, m_e; negligible d_e is adopted at early times.

The dominant cosmological observables arise in the late universe through environmental and line-of-sight temporal transport: distance probes traversing unsuppressed voids accumulate open-path temporal shear, while growth probes in dense virialized clusters are screened. This separation between homogeneous (CMB-safe) and inhomogeneous (late-time active) modes is the defining feature of the TEP cosmological implementation tested in Papers 18 and 26.

Growth and S_8

In unscreened low-density regions, the effective Newton constant is $G_{\rm eff}(k,a) = G[1 + 2\alpha_0^2/(1 + m_\phi^2 a^2/k^2)]$, giving mild scale-dependent growth, raising $f\sigma_8$ on large scales while screening suppresses changes in dense regions. A net reduction of S_8 inferred from weak lensing by ~0.01–0.03 is possible while preserving CMB lensing. Detailed MCMC fits with CLASS/HyRec and related Boltzmann-pipeline modifications have been developed and tested in the companion cosmology papers, with validation against growth, lensing, BAO, and structure-formation data.

Standard sirens

In the late-time conformal limit, EM and GW share null cones; standard siren distances are unaffected kinematically. Subtle, detector time-standard effects may introduce an integrated ϕ-history contribution at the sub-second level over ~100 Mpc; ensemble analyses can bound or detect this.

9. Quantum Clocks, Interferometry, and Composition Dependence

Quantum evolution

Proper-time Schrödinger evolution $i\hbar d|\psi\rangle/d\tau = \hat{H}|\psi\rangle$ becomes $i\hbar d|\psi\rangle/d\tilde{t} = A(\phi)\hat{H}|\psi\rangle$ in the matter frame. Transition frequencies scale as $\nu \propto A(\phi)$ with tiny sectoral corrections from dilaton-like couplings d_e, d_μ, d_q:

$$\delta \ln \nu = \delta \ln A + K_\alpha \delta \ln \alpha + K_\mu \delta \ln \mu + K_q \delta \ln X_q + \ldots \tag{59}$$

Species sensitivity

Different clock transitions carry different K-coefficients; by comparing ratios, one can disentangle the universal $A(\phi)$ scaling from composition dependence and constrain d_e, d_μ, d_q.

Interferometry

Phases acquire contributions proportional to the integral of $A(\phi)$ along arms. Atom interferometers with vertical baselines can sense $\partial_h \phi$ at 10^{-21}–10^{-22} m^{-1}; photon interferometers are sensitive at different bands.

Decoherence

Rapid ϕ variations would induce dephasing at rates $O(\partial_t \phi)$, strongly bounded by clock stabilities. Adiabatic evolution in the lab is assumed, consistent with null drift bounds.

Inset: What "no-variable-c" tests do—and don't—probe (TEP view)

Gauge-invariant observable. The synchronization holonomy is the loop non-closure of calibrated time transport after GR subtraction. Let σ denote the time-transport one-form whose line integral equals the calibrated proper-time increment along each leg. The residual holonomy is

$$H_{\rm resid}(C) \equiv \oint_C (\tilde{\sigma} - \sigma_{\rm GR}) = \iint_\Sigma (\tilde{F} - F_{\rm GR}), \tag{60}$$

the integral of the residual curvature two-form over a surface Σ bounded by the closed loop $C = \partial\Sigma$. It is built from measured proper-time increments along each leg and has units of time. Because it is the closed-loop integral of the GR-subtracted synchronization connection, $\Delta\sigma = \tilde{\sigma} - \sigma_{\rm GR}$, it is invariant under admissible synchronization re-gaugings. Re-gaugings shift both the matter-frame connection and the corresponding GR reference connection by the same exact one-form, leaving $\Delta\sigma$ invariant (since $\oint_C d\chi = 0$ for single-valued χ). It **vanishes in SR/GR and in the conformal-only limit** of TEP. The GR subtraction includes Sagnac, Lense–Thirring/gravito-magnetic, Shapiro, gravitational redshift, station motion, clock-scale realization, and reference-frame corrections, computed with ITRF ephemerides and TT/TDB standards.

How flagship constraints map to $H_{\rm resid}$:

- **GW170817 (GW–EM coincidence).** $|c_\gamma - c_g|/c \lesssim 10^{-15}$ constrains global cone splits. In TEP, late-time conformal coupling preserves null cones, so EM and GW share causal structure; small disformal tilts today are allowed. This is a boundary condition, not a loop-holonomy test.
- **Cassini (PPN-γ).** Two-way Doppler/Shapiro is reciprocity-even; it calibrates $\sigma_{\rm GR}$ to subtract but does not bound $H_{\rm resid}$.
- **Resonator MM/KT tests.** Cavities bound closed-path, even-parity (two-way sums) anisotropy at $10^{-17} - 10^{-18}$, yet are blind to odd-parity (direction-reversing one-way differences) non-reciprocity and loop non-closure—the ingredients of $H_{\rm resid}$.
- **"GPS works."** Network self-consistency uses explicit GR+Sagnac modeling and largely two-way/common-view calibration. This verifies internal consistency under assumed GR model; not a direction-reversing one-way loop-closure null.
- **Clock redshift & pairwise A↔B tests.** Exquisitely confirm GR locally; **only closed loops** (A→B→C→A with direction reversal) can reveal non-integrability captured by $H_{\rm resid}$.

Why classics can be null while $H_{\rm resid} \neq 0$:

1. Conformal null-cone invariance ⇒ no large GW–EM kinematic delays (consistent with GW170817).
2. $\partial_t\phi = 0$ **over loop timescale; gradients conservative: no first-order one-way anisotropy.** Along a fixed path, forward/back times cancel at $\mathcal{O}(B, \nabla\phi)$; leading effects are second order or require time dependence/kinematics. Thus two-way/closed-path nulls can hold while a loop-holonomy test remains sensitive.

Experimental falsifier (primary endpoints). Run a closed-loop, one-way time-transfer (and/or portable-clock) test and report:

- Leg-wise antisymmetry: $\Delta t_{AB} = t_{AB} - t_{BA}$ (and optionally $\Xi_{AB} \equiv (t_{AB} - t_{BA})/(t_{AB} + t_{BA})$).
- Loop holonomy $H_{\rm resid}$ after subtracting the full GR, kinematic, clock-scale, and instrumental synchronization model. Use triangle/quadrilateral geometries with direction reversal; extend with interplanetary one-way links and multi-species clock networks.

10. Experimental Proposals and Falsifiability

A suite of decisive, cross-checking experiments is proposed that can falsify, constrain, or provide controlled support for the theory. All observables are dimensionless ratios or calibrated residuals; all designs include nulls, blinding, and open data.

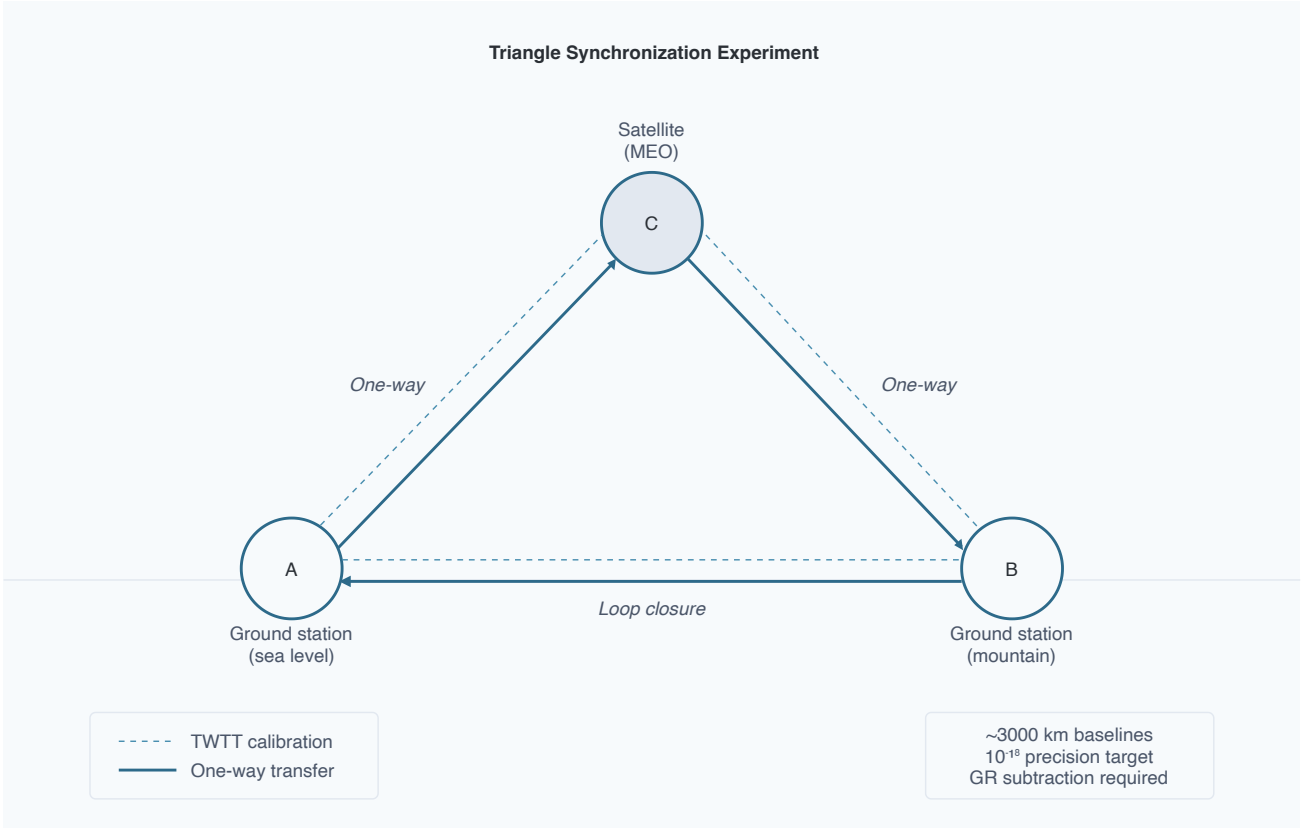

Figure 3. Triangle synchronization experiment geometry. Two ground stations (sea level and mountain) and a medium-Earth-orbit satellite form ~3000 km baselines; two-way time transfer calibrates each edge while one-way transfers around the loop probe H_{resid} after GR subtraction.

A. Triangle synchronization holonomy (ground–ground–satellite)

Geometry. Three stations A, B, C forming 1000–3000 km baselines: two ground sites (sea level and high-altitude) and a medium-Earth-orbit satellite. Optical two-way time transfer (TWTT) on each edge provides calibration; stabilized fibers and free-space optical links carry both calibration and one-way signals.

Protocol. Establish Einstein synchronization on each edge via TWTT. Execute one-way transfers around the loop in both senses at high cadence for months. Record raw timestamps, environmental monitors (pressure, temperature, humidity), refractivity profiles, TEC for ionosphere, and precise ephemerides.

Modeling. Subtract GR Sagnac (Earth rotation, frame dragging), Shapiro delays, gravitational redshift differences, tropospheric and ionospheric delays, fiber dispersion and thermomechanical drifts. Use GNSS and gravimetric models.

Observable. The measured loop residual is

$$H_{\mathrm{resid}}(C) = \oint_C (\tilde{\sigma} - \sigma_{\mathrm{GR}}) = \oint_C \Delta\sigma, \tag{61}$$

where σ_{GR} is computed from the full GR, kinematic, geodetic, atmospheric, instrumental, and clock-scale model for the same loop.

Forecast magnitude $O(10^{-18}\text{–}10^{-16})$ fraction per loop time (0.1–1 s), limited by disformal and time-varying $A(\phi)$ effects. Null in GR by design.

Error budget (fractional per loop, targets after months):
- Clock instability after averaging: 5×10^{-19}
- Two-way calibration residual: 2×10^{-19}
- Troposphere residual: 2×10^{-19}
- Fiber path noise after stabilization: 5×10^{-19}
- Ephemeris/geodesy: 2×10^{-19}
- GR subtraction residual: 5×10^{-19}
- **Total systematic floor (rss):** ~8×10^{-19}

Target: below 10^{-18}; demonstrated capability reaches 10^{-19} regime

Falsification. Null at $<1\times10^{-19}$ fractional across seasons/geometry excludes disformal/time-varying A signatures with late-time cosmological relevance.

B. Portable-clock "clock anholonomy"

Design. Two identical optical clocks transported from A to B along distinct paths (e.g., sea-level highway vs. mountain pass), durations ~1–3 days, then compared at B to a stationary clock. Common-view time transfer provides epoch.

Prediction. Path-dependent discrepancy Δ_{12} at few$\times10^{-19}$ for plausible $\alpha\dot{\phi}_0$ and $\partial_h\phi$ under screening; null at 10^{-20} bounds $\partial_t\phi$ and $\partial_h\phi$ tightly.

Systematics. Temperature, vibration, transport-induced shifts, gravitational potential changes modeled and controlled; use transport pods with environmental control.

C. Multi-species clock network: annual modulations

Network. Global network of optical clocks (Sr, Yb, Al^+, Hg^+, Ca, H(1s–2s)) cross-compared over years.

Prediction. Phase-locked annual modulations in differential ratios ν_A/ν_B with amplitudes 10^{-19}–10^{-17}, phases tied to orbital eccentricity. Species-amplitude ratios reflect $\alpha_A - \alpha_B$; a fit yields $\alpha(\phi)$ and dilaton coefficients d_e, d_μ, d_q.

Nulls. Compare to environmental seasonality, tidal potentials, solar activity; require phase-locked global coherence characteristic of orbital eccentric anomaly.

D. Interplanetary one-way optical time transfer

Design. Two drag-free spacecraft with 10^{-18}-class optical lattice clocks, separated by 1–5 AU. Optical comb-based one-way time transfer, with third node for calibration (Earth or a relay). Kinematic synchronization via slow-clock transport or common-view transponders.

Prediction. Geometry-dependent one-way asymmetry parameter $\Xi_{AB} \equiv (t_{AB} - t_{BA})/(t_{AB} + t_{BA})$ at 10^{-15}–10^{-14} (0.05–5 ps) for disformal tilts consistent with GW bounds; purely conformal temporal-variation effects are much smaller and geometry-averaging helps isolate them.

Systematics. Plasma delays, pointing jitter, thermal drifts, deep-space clock performance; anticipate >decade timeline.

E. Clock Network Correlation Analysis and Environmental Screening Maps

Objective. Detect spatial correlations and environmental screening signatures in atomic clock frequency residuals consistent with screened scalar field coupling $A(\phi)$ to transition frequencies.

Design.
Phase I - Distance Correlation Analysis:
• Analyze existing precision clock networks (GNSS, optical clock arrays) for distance-dependent correlations in frequency residuals
• Apply phase-coherent cross-spectral analysis between station pairs
• Bin pairs by 3D distance, fit exponential correlation model: $C(r) = A \cdot \exp(-r/\lambda_T) + C_0$
• Cross-validate across independent analysis centers to control systematics

Phase II - Environmental Screening Maps:
• Deploy identical optical clocks at sea-level, mountain, stratospheric balloon, and LEO; intercompare with two-way optical links

• Subtract GR redshift and Doppler shifts; correlate residuals with detailed geophysical models and gravimetry to isolate screening signatures

Forecast.
• Distance correlations: Exponential decay with characteristic length $\lambda_T \sim 2,000 - 3,000$ km for viable screening parameters
• Altitude dependence: 10^{-19}–10^{-18} frequency shifts over tens of kilometers for $\lambda_{\rm scr} \sim 10$ km near Earth
• Multi-center cross-validation expected to show <5% variation in fitted parameters

F. Multi-messenger ensemble

Design. Stack $N \gtrsim 30$ multi-messenger events with prompt EM counterparts; marginalize astrophysical lag distributions. Seek distance-correlated trends in $t_{\rm EM} - t_{\rm GW}$.

Prediction. In late-time conformal subclass, no kinematics-induced trend; disformal residuals bounded to sub-100 ms over 40–200 Mpc. Nulls constrain $B(\phi_0)(\partial\phi)^2$.

11. Statistical and Open Science Principles

Pre-registration. Publish analysis plans (models, priors, nulls, thresholds) for triangle and portable-clock experiments; record any deviations.

Blinding. Blind event-time stamps and calibration offsets; employ independent teams for calibration and analysis.

Open data/code. Release raw timestamps, environmental monitors, calibration logs, and pipelines with DOIs; release CLASS/HyRec modification, atom-sensitivity database, and meta-analytic code.

Hierarchical inference. Use heavy-tailed likelihoods (Student-t) to mitigate outliers; multi-level random effects by domain; selection models for publication bias; explicit covariance modeling for shared systematics.

12. Addressing Critiques and Clarifying Claims

No EM–GW kinematic delay in conformal subclass. With $B = 0$ today, EM and GW share null cones; any observed delays are astrophysical/source or detector-time-standard effects. Earlier overstatements are corrected and aligned with GW170817 constraints.

Static ϕ gradients do not generate first-order one-way anisotropy. An explicit derivation (Appendix A2) shows cancellation, correcting prior misinterpretations.

Holonomy invariant and not a synchronization artifact. The observable $H_{\rm resid}$ is constructed from physical proper-time measurements as the closed-loop integral of the GR-subtracted synchronization connection, $\Delta\sigma = \tilde{\sigma} - \sigma_{\rm GR}$. Synchronization re-gaugings shift both the matter-frame connection and the corresponding GR reference connection by the same exact one-form, leaving $\Delta\sigma$ and therefore $H_{\rm resid}$ invariant.

Causality and hyperbolicity. Explicit invertibility and signature conditions are given, restricting to canonical kinetics and small disformal couplings; matter-frame causality is preserved. The small-B regime is safe.

The cosmological implementation has been tested with native hi_class MCMC fits (Paper 18) and Cobaya joint-likelihood analyses (Paper 26), providing evidence that the CMB-preserving realization can respect Planck acoustic anchors while producing late-time environmental observables.

13. Philosophical and Conceptual Implications

Simultaneity beyond Einstein. Special relativity makes simultaneity observer-dependent; dynamic time makes synchronization non-integrable at the global scale. The invariant content is a holonomy of time transport: moving clocks around closed loops in a dynamical time background returns path-dependent offsets after subtracting GR effects.

Constants clarified. The speed of light is an invariant in local tangent spaces; globally, "c" is not a number but a family of operational ratios dependent on clock histories in a time field. Variation of constants becomes a question about dimensionless ratios across environments and epochs.

Machian undertone. The rate of time responds weakly to the stress-energy of matter through αT, giving a principled, covariant flavor to the idea that the "rest of the universe" influences local rates, without violating local physics.

14. Conclusions

This paper articulates a covariant framework in which the rate of time is a dynamical field with universal matter coupling. The architecture preserves local Lorentz invariance and null-cone structure (in the conformal limit), conforms to multi-messenger bounds, and yields new invariant observables—synchronization holonomy and clock anholonomy—that vanish in GR and are measurable with modern clocks. Screening reconciles local nulls with cosmological dynamics; a controlled disformal sector allows minute, bounded photon-cone tilts that provide clean targets for holonomy experiments. The theory is falsifiable with realistic experiments and promises to clarify persistent cosmological tensions.

Einstein moved us from absolute time to relative simultaneity and dynamic geometry. The next step is to recognize that the flow of time itself is dynamical, and that "the speed of light" is the local echo of a deeper temporal geometry. If the predicted holonomies are observed, physics will enter a new epoch in which dynamic time joins dynamic geometry as a foundation. If not, uniquely strong bounds will have been set and the operational bedrock of c and simultaneity clarified to unprecedented precision.

Appendix A: Proofs and Key Derivations

A1. Conformal null-cone invariance

Let $\tilde{g}_{\mu\nu} = A(\phi)^2 g_{\mu\nu}$ with $A > 0$. A vector k^μ null with respect to $g_{\mu\nu}$, $g_{\mu\nu}k^\mu k^\nu = 0$, satisfies $\tilde{g}_{\mu\nu}k^\mu k^\nu = A^2 g_{\mu\nu}k^\mu k^\nu = 0$. Maxwell's action $S = -(1/4)\int \sqrt{-g}F_{\mu\nu}F^{\mu\nu}$ is conformally invariant in 4D: under $\tilde{g}_{\mu\nu} = \Omega^2 g_{\mu\nu}$, $\sqrt{-\tilde{g}}F_{\mu\nu}F^{\mu\nu} = \sqrt{-g}F_{\mu\nu}F^{\mu\nu}$. Hence photon geodesics are conformally invariant; null cones coincide.

A2. No first-order one-way anisotropy in static φ

Consider a straight path $x(s)$ along $\nabla\phi$ with $s \in [0, L]$. Expand $A(\phi(s)) = 1 + \alpha\phi(s) + O(\alpha^2)$.

Forward time. Parameterize $s = 0 \to L$ with $\phi(s) = \phi_0 + s\,\partial_\parallel\phi$:

$$t_\rightarrow = \frac{1}{c}\int_0^L \big[1 + \alpha(\phi_0 + s\,\partial_\parallel\phi)\big]\,ds = \frac{L}{c} + \frac{\alpha}{c}\Big(\phi_0 L + \frac{1}{2}L^2\,\partial_\parallel\phi\Big). \tag{62}$$

Backward time. Parameterize $s' = 0 \to L$ with $\phi(s') = \phi_1 - s'\,\partial_\parallel\phi$, where $\phi_1 = \phi_0 + L\,\partial_\parallel\phi$:

$$t_\leftarrow = \frac{1}{c}\int_0^L \big[1 + \alpha(\phi_1 - s'\,\partial_\parallel\phi)\big]\,ds' = \frac{L}{c} + \frac{\alpha}{c}\Big(\phi_1 L - \frac{1}{2}L^2\,\partial_\parallel\phi\Big). \tag{63}$$

Substituting $\phi_1 = \phi_0 + L\,\partial_\parallel\phi$,

$$t_\leftarrow = \frac{L}{c} + \frac{\alpha}{c}\Big(\phi_0 L + L^2\,\partial_\parallel\phi - \frac{1}{2}L^2\,\partial_\parallel\phi\Big) = \frac{L}{c} + \frac{\alpha}{c}\Big(\phi_0 L + \frac{1}{2}L^2\,\partial_\parallel\phi\Big) = t_\rightarrow. \tag{64}$$

Thus $t_\rightarrow - t_\leftarrow = 0 + O((\partial\phi)^2, \alpha^2)$. The first nonzero term is second order.

A3. Synchronization holonomy invariance and projected disformal connection

This appendix derives the leading-order disformal contribution to the synchronization connection used in Section 7 and shows why the GR-subtracted closed-loop residual is invariant under synchronization re-gauging.

A3.1 Synchronization connection and re-gauging

Consider a local threading decomposition of the matter-frame metric relative to a physical clock-network congruence:

$$d\tilde{s}^2 = \tilde{g}_{00}\big(dt + \tilde{\sigma}_i dx^i\big)^2 + \tilde{h}_{ij}dx^i dx^j. \tag{65}$$

Equivalently, up to the sign convention used for $\tilde{\sigma}_i$,

$$\tilde{\sigma}_i = \frac{\tilde{g}_{0i}}{\tilde{g}_{00}}. \tag{66}$$

If the opposite sign convention is adopted, all shifts below acquire the opposite sign, but the closed-loop result is unchanged.

A synchronization re-gauging of the same physical clock network assigns a different simultaneity offset to the same clock worldlines:

$$t' = t + \chi(x^i), \tag{67}$$

where χ is a single-valued spatial clock-offset function on the network at the epoch of the loop measurement. Then

$$dt = dt' - \partial_i \chi \, dx^i. \tag{68}$$

Substituting into the metric gives

$$dt + \tilde{\sigma}_i dx^i = dt' + (\tilde{\sigma}_i - \partial_i \chi) dx^i. \tag{69}$$

Therefore

$$\tilde{\sigma}_i \longrightarrow \tilde{\sigma}'_i = \tilde{\sigma}_i - \partial_i \chi. \tag{70}$$

In one-form notation,

$$\tilde{\sigma} \longrightarrow \tilde{\sigma} - d\chi. \tag{71}$$

With the opposite sign convention for $\tilde{\sigma}$, the sign reverses. In either convention, the change is exact.

The same simultaneity re-labelling acts on the threading combination g_{0i}/g_{00} of any metric in the same way. The GR reference connection σ_{GR} is the corresponding threading connection computed from the GR reference metric on the same physical clock-network congruence, with the same loop, same coordinate convention, and the standard Sagnac, Lense--Thirring, Shapiro, gravitational-redshift, station-motion, clock-scale, and reference-frame corrections included. Therefore the same re-labelling gives

$$\sigma_{\mathrm{GR}} \longrightarrow \sigma_{\mathrm{GR}} - d\chi. \tag{72}$$

The GR-subtracted residual connection

$$\Delta\sigma \equiv \tilde{\sigma} - \sigma_{\mathrm{GR}} \tag{73}$$

therefore transforms as

$$\Delta\sigma \longrightarrow (\tilde{\sigma} - d\chi) - (\sigma_{\mathrm{GR}} - d\chi) = \Delta\sigma. \tag{74}$$

Thus the closed-loop observable

$$H_{\mathrm{resid}}(C) = \oint_C \Delta\sigma \tag{75}$$

is invariant under synchronization re-gauging.

Equivalently, if one works with a representative in which the residual connection itself shifts by an exact form,

$$\Delta\sigma \to \Delta\sigma + d\chi_{\mathrm{res}}, \tag{76}$$

then the loop integral is still invariant because

$$\oint_C d\chi_{\mathrm{res}} = 0 \tag{77}$$

for single-valued χ_{res}. The observable is the loop class of the residual connection modulo exact one-forms, not a raw one-way synchronization convention.

This proof is local in time. The loop C is evaluated on the spatial network at a specified epoch. Time dependence of ϕ, $B(\phi)$, or the matter metric may change the value of $\Delta\sigma$ from one epoch to another, but it does not change the synchronization-gauge argument at a fixed epoch. The gauge freedom relevant to the closed-loop observable is the spatial simultaneity re-labelling $\chi(x^i)$ of the specified physical clock network.

A3.2 Projected disformal contribution

The matter metric is

$$\tilde{g}_{\mu\nu} = A^2(\phi) g_{\mu\nu} + B(\phi) \nabla_\mu \phi \nabla_\nu \phi. \tag{78}$$

Let u^μ be the four-velocity of the physical clock network defining the synchronization protocol, with

$$u^\mu u_\mu = -1 \tag{79}$$

in the $(-+++)$ signature. The spatial projector into the local rest space of this congruence is

$$P_\mu{}^\nu = \delta_\mu{}^\nu + u_\mu u^\nu. \tag{80}$$

The scalar gradient decomposes as

$$\nabla_\mu \phi = D_\mu \phi - (u \cdot \nabla \phi) u_\mu, \tag{81}$$

where

$$D_\mu \phi = P_\mu{}^\nu \nabla_\nu \phi \tag{82}$$

is the spatial gradient measured by the clock network.

The disformal part of the matter metric is

$$\delta_B \tilde{g}_{\mu\nu} = B \nabla_\mu \phi \nabla_\nu \phi. \tag{83}$$

Its mixed time-space projection relative to the clock-network congruence is

$$P_\mu{}^\alpha u^\beta \delta_B \tilde{g}_{\alpha\beta} = B\,(P_\mu{}^\alpha \nabla_\alpha \phi)\,\big(u^\beta \nabla_\beta \phi\big), \tag{84}$$

so

$$P_\mu{}^\alpha u^\beta \delta_B \tilde{g}_{\alpha\beta} = B D_\mu \phi (u \cdot \nabla \phi). \tag{85}$$

The synchronization connection is the normalized mixed time-space component of the matter metric. In a local rest frame of the clock congruence, the conformal background gives

$$\tilde{g}^{(A)}_{00} = -A^2, \tag{86}$$

while the disformal correction gives

$$\delta_B \tilde{g}_{0i} = B (u \cdot \nabla \phi) D_i \phi. \tag{87}$$

The disformal sector also corrects $\tilde{g}_{00}$ at order $B(u \cdot \nabla \phi)^2$. However, in the local rest frame of the clock congruence the conformal background has no mixed time-space component, $\tilde{g}^{(A)}_{0i} = 0$. Therefore the correction to $1/\tilde{g}_{00}$ multiplies a vanishing conformal numerator and first contributes only at higher order in B. To leading order, the denominator may consistently be evaluated at $\tilde{g}^{(A)}_{00} = -A^2$.

Therefore, to leading order in B, using the convention $\tilde{\sigma}_i = \tilde{g}_{0i}/\tilde{g}_{00}$,

$$\delta\tilde{\sigma}_i \simeq \frac{\delta_B \tilde{g}_{0i}}{\tilde{g}^{(A)}_{00}} \simeq -\frac{B}{A^2} (u \cdot \nabla \phi) D_i \phi. \tag{88}$$

With the opposite convention for the synchronization one-form, the overall sign is reversed; the closed-loop invariance and exact/non-exact distinction are unaffected.

In covariant projected form this is

$$\delta\tilde{\sigma}_\mu \simeq -\frac{B}{A^2} (u \cdot \nabla \phi) D_\mu \phi, \tag{89}$$

or equivalently

$$\delta\tilde{\sigma}_\mu \simeq -\frac{B}{A^2} (u \cdot \nabla \phi) P_\mu{}^\nu \nabla_\nu \phi. \tag{90}$$

Higher-order terms include corrections from the disformal contribution to $\tilde{g}_{00}$, lapse-shift mixing, and higher powers of $B(\nabla\phi)^2/A^2$.

In a hypersurface-orthogonal $3+1$ slicing, where $u^\mu = n^\mu$, this reduces to

$$\delta\tilde{\sigma}_i \approx -\frac{B}{A^2 N} (\partial_i \phi)(n \cdot \partial \phi), \tag{91}$$

up to lapse-shift convention and higher-order disformal corrections.

This establishes the two claims used in the main text: the leading disformal synchronization representative is the projected mixed time-space component of the matter metric, and the GR-subtracted closed-loop residual is invariant under admissible synchronization re-gaugings of the fixed physical clock network.

A4. Disformal inverse and causality condition

Given $\tilde{g}_{\mu\nu} = A^2 g_{\mu\nu} + B\partial_\mu\phi\partial_\nu\phi$, define the scalar-gradient one-form $q_\mu \equiv \partial_\mu\phi$. The inverse satisfies $\tilde{g}^{\mu\nu}\tilde{g}_{\nu\sigma} = \delta^\mu_\sigma$. Ansätz: $\tilde{g}^{\mu\nu} = A^{-2}(g^{\mu\nu} + Cq^\mu q^\nu)$. Solve for C:

$$A^{-2}[g^{\mu\nu} + Cq^\mu q^\nu][A^2 g_{\nu\sigma} + Bq_\nu q_\sigma] = \delta^\mu_\sigma \tag{92}$$

$$\Rightarrow \delta^\mu_\sigma + A^{-2}(B + A^2 C + BC(q\cdot q))q^\mu q_\sigma = \delta^\mu_\sigma \tag{93}$$

$$\Rightarrow A^2 C + B + BC(q\cdot q) = 0 \Rightarrow C = -\frac{B}{A^2 + B(q\cdot q)}. \tag{94}$$

Thus $\tilde{g}^{\mu\nu} = A^{-2}\left[g^{\mu\nu} - \frac{(B/A^2)q^\mu q^\nu}{1+(B/A^2)(q\cdot q)}\right]$. Lorentzian signature requires $1 + (B/A^2)(q\cdot q) > 0$.

Appendix B: Photon Phase Speed and GW–EM Constraints

In a local inertial frame ($g_{\mu\nu} = \eta_{\mu\nu}$), the photon dispersion relation is $\tilde{g}^{\mu\nu}k_\mu k_\nu = 0$. Using the disformal inverse from A4,

$$\eta^{\mu\nu}k_\mu k_\nu = \frac{(B/A^2)(q\cdot k)^2}{1 + (B/A^2)(q\cdot q)}. \tag{95}$$

For a photon with 4-momentum $k^\mu = (\omega/c)(1,\hat{n})$, and a static scalar gradient $q_\mu = (0, \nabla\phi)$, $q\cdot k = (\omega/c)\,\partial_{\hat{n}}\phi$ and $q\cdot q = |\nabla\phi|^2$. Hence

$$-\frac{\omega^2}{c^2} + |\vec{k}|^2 = \frac{(B/A^2)(\omega/c)^2(\partial_{\hat{n}}\phi)^2}{1 + (B/A^2)|\nabla\phi|^2}. \tag{96}$$

The phase speed $v_{\rm ph} = \omega/|\vec{k}|$ is therefore

$$v_{\rm ph} = c\left[1 + \frac{(B/A^2)(\partial_{\hat{n}}\phi)^2}{1 + (B/A^2)|\nabla\phi|^2}\right]^{-1/2} \approx c\left[1 - \frac{1}{2}\frac{(B/A^2)(\partial_{\hat{n}}\phi)^2}{1 + (B/A^2)|\nabla\phi|^2}\right]. \tag{97}$$

Gravitons propagate on $g_{\mu\nu}$, so $c_g = c$ exactly. The maximal fractional speed difference between photons and gravitons, for propagation perpendicular to $\nabla\phi$ ($\partial_{\hat{n}}\phi = 0$) versus along it ($\partial_{\hat{n}}\phi = |\nabla\phi|$), is bounded by the disformal term:

$$\frac{|c_\gamma - c_g|}{c} \lesssim \frac{1}{2}\frac{(B/A^2)|\nabla\phi|^2}{1 + (B/A^2)|\nabla\phi|^2} \approx \frac{B}{2A^2}|\nabla\phi|^2 \quad (\text{for small } B). \tag{98}$$

The GW170817/GRB170817A bound $|c_\gamma - c_g|/c \lesssim \text{few} \times 10^{-15}$ therefore requires

$$\frac{B(\phi)}{A(\phi)^2}\,|\nabla\phi|^2 \lesssim \text{few} \times 10^{-15} \tag{99}$$

along typical lines of sight today, bounding the present-day disformal coupling $B(\phi_0)$.

Appendix C: Glossary of Symbols

Symbol	Description	Section
$g_{\mu\nu}$	Gravitational metric tensor	2
$\tilde{g}_{\mu\nu}$	Matter/causal metric tensor	2
ϕ	The scalar time field	2
$A(\phi)$	Conformal coupling factor, $\exp(\beta_A \phi / M_{\rm Pl})$	2
$B(\phi)$	Disformal coupling function	2
TEP	Temporal Equivalence Principle	1, 2
τ	Proper time defined by $\tilde{g}_{\mu\nu}$	2
$H_{\rm resid}$	residual synchronization holonomy, $H_{\rm resid}(C) \equiv \oint_C (\tilde{\sigma} - \sigma_{\rm GR})$	3, 6
$\Delta\sigma$	GR-subtracted synchronization connection, $\Delta\sigma \equiv \tilde{\sigma} - \sigma_{\rm GR}$	3, 6, 7, A3
u^μ, u_μ	four-velocity field of the physical clock-network congruence (upper index contravariant, lower index covariant)	3, 7, A3
$P_\mu{}^\nu$	spatial projector into the local rest space of the clock-network congruence, $P_\mu{}^\nu = \delta_\mu{}^\nu + u_\mu u^\nu$ in $(-+++)$ signature	7, A3
q_μ	scalar-gradient one-form, $q_\mu \equiv \partial_\mu \phi$	A4, B
c_g, c_γ	Speed of gravity, speed of light (photons)	5
$V(\phi)$	Potential for the scalar field ϕ	4
$\alpha(\phi)$	Conformal coupling strength, $d(\ln A)/d\phi$	4
β_A	Dimensionless conformal coupling parameter	2
M	Suppression scale for disformal/EFT operators	4
PPN	Parametrized Post-Newtonian formalism	7
$\gamma_{\rm PPN}$, $\beta_{\rm PPN}$	Eddington PPN parameters	7
H_0	Hubble constant today	9
S_8	Cosmological parameter for structure growth	9
r_s	Sound horizon at recombination	9
Ξ_{AB}	One-way time asymmetry between A and B	6.4
k^μ	Four-wavevector of a null signal	3.2
$\ln A(\phi)$	conformal factor controlling matter-frame proper time; compact notation $\Theta \equiv \ln A$	7
Σ_μ	Temporal Shear vector, $\Sigma_\mu \equiv \nabla_\mu \ln A(\phi)$	7
C_A	covariance of conformal-factor fluctuations, $C_A(x,x') = \langle \delta \ln A(x)\, \delta \ln A(x') \rangle$; also denoted C_Θ when using $\Theta \equiv \ln A$	7
λ_T	Temporal Topology correlation length measured in clock/covariance data	7
ρ_T	Temporal Topology saturation scale; not a binary ambient-density switch	7
κ_X	Observable response coefficient for channel X, not a microscopic coupling	7

References

Einstein, A. (1905). Zur Elektrodynamik bewegter Körper. Ann. Phys. 17, 891–921.

Einstein, A. (1916). Die Grundlage der allgemeinen Relativitätstheorie. Ann. Phys. 49, 769–822.

Will, C. M. (2014). The Confrontation between General Relativity and Experiment. Living Rev. Relativity 17, 4.

Bertotti, B., Iess, L. & Tortora, P. (2003). A test of general relativity using radio links with the Cassini spacecraft. Nature 425, 374–376.

Bekenstein, J. D. (1993). The relation between physical and gravitational geometry. Phys. Rev. D 48, 3641.

Damour, T. & Polyakov, A. M. (1994). The string dilaton and a least coupling principle. Nucl. Phys. B 423, 532.

Khoury, J. & Weltman, A. (2004). Chameleon fields: Awaiting surprises for tests of gravity in space. Phys. Rev. Lett. 93, 171104.

Hinterbichler, K. & Khoury, J. (2010). Symmetron fields. Phys. Rev. Lett. 104, 231301.

Abbott, B. P. et al. (LIGO/Virgo) (2017). GW170817: Observation of gravitational waves from a binary neutron star inspiral. Phys. Rev. Lett. 119, 161101.

Abbott, B. P. et al. (2017). Multi-messenger observations of a binary neutron star merger. ApJ 848, L12.

Planck Collaboration (2020). Planck 2018 results. VI. Cosmological parameters. A&A 641, A6.

Riess, A. G. et al. (2022). A comprehensive measurement of the local value of the Hubble constant. ApJ 934, L7.

Bothwell, T. et al. (2022). JILA Sr optical lattice clock with 10−18 stability and accuracy. Nature 602, 420–424.

Touboul, P. et al. (2022). MICROSCOPE mission: test of the equivalence principle in space. Phys. Rev. Lett. 129, 121102.

Burrage, C. & Sakstein, J. (2018). Tests of chameleon gravity. Living Rev. Relativity 21, 1.

Bettoni, D. & Liberati, S. (2013). Disformal invariance of second-order scalar-tensor theories. Phys. Rev. D 88, 084020.

Koivisto, T. S. & Zumalacárregui, T. (2013). Disformal gravity. Phys. Rev. D 88, 084016.

Ashby, N. (2003). Relativity in the Global Positioning System. Living Rev. Relativity 6, 1.

Uzan, J.-P. (2011). Varying constants, gravitation and cosmology. Living Rev. Relativity 14, 2.

Michelson, A. A. & Morley, E. W. (1887). On the relative motion of the Earth and the luminiferous ether. Am. J. Sci. 34, 333–345.

Kennedy, R. J. & Thorndike, E. M. (1932). Experimental establishment of the relativity of time. Phys. Rev. 42, 400–418.

Müller, H. et al. (2003). Modern Michelson-Morley experiment using cryogenic optical resonators. Phys. Rev. Lett. 91, 020401.

Herrmann, S. et al. (2009). Test of the isotropy of the speed of light using a continuously rotating optical resonator. Phys. Rev. Lett. 95, 150401.

IERS Conventions (2010). Gérard Petit and Brian Luzum (eds.). IERS Technical Note No. 36, Frankfurt am Main: Verlag des Bundesamts für Kartographie und Geodäsie.

How to cite

You can cite all versions by using the DOI: 10.5281/zenodo.16921911

BibTeX:

```
@misc{Smawfield_TEP_2025,
  author       = {Matthew Lukin Smawfield},
  title        = {Temporal Equivalence Principle: Dynamic Time &
                  Emergent Light Speed},
  year         = {2025},
  publisher    = {Zenodo},
  doi          = {10.5281/zenodo.16921911},
  url          = {https://doi.org/10.5281/zenodo.16921911},
  note         = {Preprint}
}
```

Contact

For questions, comments, or collaboration opportunities regarding this work, please contact:

Matthew Lukin Smawfield
✉ *matthew@mlsmawfield.com*